

1           **Streptolysin production and activity is central to *in vivo* pathotype and**  
2                                   **disease outcome in GAS infections**  
3

4   Jenny Clarke<sup>1</sup>, Murielle Baltazar<sup>1\*</sup>, Mansoor Alshahag<sup>1,3\*</sup>, Stavros Panagiotou<sup>1</sup>, Marion Pouget<sup>1</sup>,  
5   William A Paxton<sup>1</sup> Georgios Pollakis<sup>1</sup>, Dean Everett<sup>2</sup>, Neil French<sup>1,2¶</sup>, Aras Kadioglu<sup>1,¶\*</sup>

6  
7   <sup>1</sup>Department of Clinical Immunology, Microbiology and Immunology, Institute of Infection  
8   and Global Health, University of Liverpool, Liverpool, UK; <sup>2</sup>Malawi-Liverpool-Wellcome  
9   Trust Clinical Research Programme, Queen Elizabeth Central Hospital, Blantyre, Malawi. <sup>3</sup>  
10   Applied Medical Sciences, University of Al Baha, Saudi Arabia.

11  
12   \* These authors contributed equally

13   ¶ Co-senior authors.

14  
15  
16   \* Corresponding author:

17   Prof. Aras Kadioglu

18   Department of Clinical Immunology, Microbiology and Immunology, Institute of Infection and  
19   Global Health, University of Liverpool, Liverpool, UK

## 27 **Abstract**

28 Streptococcus pyogenes (GAS) is among the most diverse of all human pathogens, responsible  
29 for a range of clinical manifestations, from mild superficial infections such as pharyngitis to  
30 serious invasive infections such as necrotising fasciitis and sepsis. The drivers of these different  
31 disease phenotypes are not known. The GAS cholesterol-dependent cytolysin, streptolysin O  
32 (SLO), has well established cell and tissue destructive activity. We investigated the role of SLO  
33 in determining disease outcome *in vivo*, by using two different clinical lineages; the recently  
34 emerged hypervirulent outbreak *emm* type 32.2 strains, which result in sepsis, and the *emm*  
35 type 1.0 strains which cause septic arthritis. Using clinically relevant *in vivo* mouse models of  
36 sepsis and a novel septic arthritis model, we demonstrated that the amount and activity of SLO  
37 is vital in determining the pathotype of infection. The *emm*32.2 strain produced large quantities  
38 of highly haemolytic SLO that resulted in rapid development of sepsis. By contrast, the lower  
39 levels and haemolytic activity of *emm*1.0 SLO led to translocation of bacteria to joints.  
40 Importantly, sepsis associated strains that were attenuated by deletion or inhibition of SLO also  
41 translocated to the joint, confirming the key role of SLO in determining infection niche. Our  
42 findings demonstrate that SLO is key to *in vivo* pathotype and disease outcome. Careful  
43 consideration should be given to novel therapy or vaccination strategies that target SLO. Whilst  
44 neutralising SLO activity may reduce severe invasive disease, it has the potential to promote  
45 chronic inflammatory conditions such as septic arthritis.

46

47

48

49

50

51

## 52 **Introduction**

53 Group A *Streptococcus* (GAS), also called *Streptococcus pyogenes*, is a commensal of the  
54 human upper respiratory tract and also an important human pathogen, accounting for over 750  
55 million infections every year<sup>1,2</sup>. GAS is able to produce a variety of pyogenic infections that  
56 range in severity and prevalence<sup>3-5</sup>. Diseases include pharyngitis, impetigo, cellulitis and more  
57 life threatening infections such as streptococcal toxic shock syndrome, necrotising fasciitis, and  
58 sepsis<sup>3,6</sup>. The mechanisms that allow GAS to cause such diversity in disease types are  
59 unknown, however a number of studies have shown that bacterial and host-specific components  
60 may be involved<sup>7</sup>.

61

62 GAS strains are typed based on the sequence of the *emm* gene, which encodes the M-protein,  
63 of which there are over 200 known *emm* types<sup>8</sup>. The epidemiology of GAS infections has been  
64 changing globally over the last decade, with the emergence of new *emm* types and localised  
65 outbreaks a main feature<sup>9</sup>. Within *emm* types of GAS, isolates may be causative of a range of  
66 clinical outcomes, such that most lineages carry the potential for expression of a range of  
67 phenotypes that may determine the course and nature of infection. Recent studies have shown  
68 distinct correlations between the host niche of recovered GAS clinical isolates and their ability  
69 to secrete high concentrations of known virulence factors such as streptococcal pyrogenic  
70 exotoxin A, B, and C (SpeA, SpeB, and SpeC), or the haemolytic exotoxin streptolysin O  
71 (SLO)<sup>10-12</sup>. In addition to this, the premise that GAS phenotypic heterogeneity contributes to  
72 distinct clinical phenotypes is supported by studies that have found changes in virulence factor  
73 production such as in streptokinase and capsular protein secretion after GAS is passaged either  
74 *ex vivo* or *in vivo*<sup>13-17</sup>.

75

76 The haemolysin SLO is well established as having cell and tissue destructive activity, and is  
77 part of the family of cholesterol dependent cytotoxins that also includes perfringolysin,  
78 pneumolysin, and listeriolysin O<sup>18-20</sup>. SLO is a highly conserved protein secreted by nearly all  
79 clinical isolates of GAS, and acts against a wide number of eukaryotic cell types including  
80 macrophages, neutrophils, and erythrocytes, by interacting with cholesterol in target cell  
81 membranes to form pores, with sufficiently high doses of SLO resulting in complete cell lysis  
82<sup>5,21-23</sup>. SLO has a number of other biological effects on the host that act at different stages  
83 throughout infection, such as its ability to cause hyper-stimulation and cell-mediated apoptosis  
84 of host immune cells such as neutrophils<sup>11,24</sup>. Although most GAS isolates have the gene for  
85 SLO, the production of SLO is heavily regulated, as shown in studies that have seen variation  
86 in cytotoxicity within and between *emm* types<sup>25</sup>. Early studies with SLO demonstrated that the  
87 purified toxin was lethal to mice and rabbits when injected intravenously, mainly due to  
88 cardiotoxicity<sup>26,27</sup>. More recently, there have been studies to assess the effects of biologically  
89 relevant concentrations of SLO in *in vivo* models. Limbago *et al.*, found that SLO-deficient  
90 GAS resulted in attenuated skin infections and similarly Zhu *et al.*, reported a reduction in  
91 virulence when using SLO-deficient GAS in an invasive wound infection model<sup>28,29</sup>.

92

93 Despite all this however, substantial gaps still exist in our understanding of the contributory  
94 role of the variation and amount of SLO production to overall GAS pathogenesis. In order to  
95 address this, we developed a custom made ELISA to compare the production of SLO between  
96 a recently emerged hypervirulent outbreak strain (which resulted in an epidemic in Liverpool,  
97 UK, between 2010-2012) characterised as *emm* type 32.2 and invasive *emm* type 1.0. isolates  
98<sup>30</sup>. Using *in vivo* GAS bacteraemia and novel septic arthritis models, we further investigated  
99 the role of SLO in establishing and maintaining different clinical pathotypes *in vivo*. In

100 addition, we investigated the role of SLO in these models, by use of a SLO deficient mutant  
101 strain in the background of the invasive outbreak *emm* type 32.2 isolate.

102

## 103 **Results**

### 104 ***In vitro* phenotypic analysis of invasive and non-invasive *emm* type strains**

105 Capsule thickness, complement deposition, and opsonophagocytic killing by macrophages was  
106 measured across 24 individual GAS isolates, covering 4 different *emm* types. Differences in  
107 capsule thickness, complement deposition, and opsonophagocytosis varied between and within  
108 *emm* type isolates. In general, invasive *emm* type 32.2 isolates had thicker capsules than non-  
109 invasive isolates (regardless of *emm* type) (Figure 1A) and had less complement deposited on  
110 their surface (Figure 1B). The size of the capsule and complement deposition were inversely  
111 proportional, with thinner capsule isolates exhibiting more complement deposition on their  
112 surface. The Pearson correlation coefficient ( $r$ ) after  $\log_{10}$  transformation was  $-0.5845$  ( $r^2 =$   
113  $0.3416$ ;  $p = 0.0027$ ). The mean percentage of killing by macrophages in *emm* type 32.2 isolates  
114 (30% killing) was marginally lower than non *emm* type 32.2 isolates (37% killing) (Figure 1C).  
115 Although there was no significant correlation between capsule thickness and  
116 opsonophagocytosis, there was a positive association between the two ( $r = 0.20$ ).

117

118 Based on these results, we chose representative isolates from the *emm* type 32.2 outbreak  
119 strains (isolate 112327) and *emm* type 1.0 strains (isolate 101910) which were most  
120 significantly different in capsule thickness, complement deposition and phagocytic killing  
121 scales, to use in subsequent *in vivo* infection modelling. As such, both isolates were from an  
122 invasive clinical phenotype but had significantly distinct phenotypic differences, with the *emm*  
123 type 32.2 isolate 112327 exhibiting a significantly thicker capsule, lower complement  
124 deposition and more resistance to killing in comparison to the *emm* type 1.0 isolate 101910.

125 ***In vivo* characterisation of *emm* type 1.0 and 32.2 isolates in models of invasive GAS**  
126 **infection**

127 An invasive GAS model was used to compare the virulence of *emm* type 1.0 (isolate 101910)  
128 and *emm* type 32.2 (isolate 112327) *in vivo*. Following intravenous infection, 100% of mice  
129 infected with isolate 112327 at  $10^8$  CFU succumbed to infection by 24 h post-infection. When  
130 infected with a ten fold lower dose of  $10^7$  CFU, all mice showed signs of lethargy by 24 h and  
131 succumbed to infection by 36 h post-infection (Figure 2A). In contrast, none of the mice  
132 infected with either  $10^8$  or  $10^7$  CFU of isolate 101910 showed any signs of infection and all  
133 survived (Figure 2A). In time point experiments over 48 h, mice infected with  $10^8$  CFU of  
134 isolate 112327 had significantly higher bacterial loads in the blood at all time points post  
135 infection in comparison to those infected with isolate 101910, this was also the case by 24 h  
136 for isolate 112327 infected at tenfold lower ( $10^7$ ) CFU dose, suggesting that overall, *emm* type  
137 32.2 (isolate 112327) is better adapted to survival and proliferation in blood.

138

139 There was no detectable CFU of isolate 101910 in blood by 24 h (at  $10^8$  dose) and by 48 h (at  
140  $10^7$  dose), demonstrating a clear difference in blood survival (Figure 2B) suggesting that *emm*  
141 type 1.0 (isolate 101910) was either less well adapted to survive in blood or was able to rapidly  
142 translocate elsewhere. Indeed, mice infected with isolate 101910 began to show symptoms of  
143 joint deformities by 24 h, which progressed until the end of the experiment. Bacteria were  
144 recovered from the knee joints at a mean log 2.4 CFU/knee joint as early as 6h (Figure 2C),  
145 and the bacterial load continued to increase up to a mean log 5.2 CFU/knee joint by the end of  
146 the experiment (day 7) (Figure 2C).

147

148

149 **Comparison of SLO production and activity in *emm* type 1.0 and 32.2 isolates**

150 To explain the clear differences in overall mouse survival, bacterial virulence and proliferation  
151 in blood between the two *emm* type 1.0 and 32.2 isolates, we quantified the amount of SLO  
152 secreted by each isolate *in vitro* (at equivalent CFU) by analysing the amount of SLO directly  
153 secreted into the supernatant by the bacteria during growth phase in planktonic culture. The  
154 concentration (ng/ml) of SLO produced by *emm* type 32.2 (isolate 112327) increased rapidly  
155 over time compared with *emm* type 1.0 (isolate 101910); whereby isolate 112327 produced  
156 significantly more SLO from 6 h onwards until the final time point at 12 h ( $p = 0.015 -$   
157  $<0.0001$ ). Isolate 101910 produced a small amount of SLO initially but the concentration did  
158 not continue to increase beyond 8 h (Figure 3A). We next looked at the haemolytic activity of  
159 SLO. The haemolytic activity of SLO secreted by isolates 112327 and 101910 followed the  
160 same pattern as that of the amount secreted; isolate 112327 SLO was significantly more  
161 haemolytic from 6 h until the final time point at 12 h compared to isolate 101910 SLO ( $p =$   
162  $0.028 - <0.0001$ ) (Figure 3B). Hence, *emm* type 32.2 (isolate 112327) secreted not only  
163 significantly more SLO than *emm* type 1.0 (isolate 101910), but also significantly more  
164 haemolytic toxin at equivalent CFU. The CFU growth of both isolates was assessed to ensure  
165 the differences observed for SLO were not due to significant differences in bacterial growth.  
166 We found no significant difference in bacterial growth for both isolates across all time points,  
167 with almost identical CFU loads at 10 and 12 h (Figure 2C), which interestingly were the same  
168 time points with the greatest difference in SLO concentration and activity, suggesting that  
169 bacterial growth rate and CFU load were not responsible for observed SLO differences between  
170 isolates.

171

172

173 ***In vivo* recovered *emm* type 1.0 (isolate 101910) has reduced production and activity of**  
174 **SLO**

175 To further clarify the reasons for *emm* type 1.0 (isolate 101910) clearance from bloodstream  
176 and translocation to the knee joints, we recovered bacteria from mouse knee joints at 24 h post  
177 infection, and quantified the amount of SLO secreted into the supernatant over an *in vitro*  
178 growth phase. We found that *in vivo* recovered isolate 101910 secreted significantly less SLO  
179 into the supernatant over the 12 h *in vitro* growth phase. There was significantly less SLO  
180 secreted from 6 h onward to that originally produced by isolate 101910 grown *in vitro* at  
181 equivalent CFU ( $p = 0.009 - <0.0001$ ) (Figure 4A). In addition to producing significantly less  
182 SLO, the haemolytic activity of *in vivo* recovered bacterial SLO was also significantly lower  
183 from 6 h to 10 h, again at equivalent CFU ( $p = 0.0007 - <0.0001$ ), with SLO activity  
184 comparable at 12 h (Figure 4B). We next wanted to determine whether *in vivo* recovered isolate  
185 101910 retained its low SLO production and low SLO activity phenotype when grown over  
186 multiple times *in vitro*. Interestingly, after just one growth phase in THYG culture, the  
187 concentration of SLO reverted to a high SLO production phenotype ( $p = <0.0001$ ) (Figure 4C),  
188 with significantly increased haemolytic activity from 6 h to 10 h ( $p = <0.005$ ) (Figure 4D),  
189 suggesting that factors *in vivo* caused isolate 101910 to suppress its SLO production. During  
190 intravenous infection with *in vivo* recovered isolate 101910 ( $10^7$  CFU), bacteria enter the knee  
191 joint at higher bacterial numbers and proliferate in the joint more quickly. These results suggest  
192 that *in vivo* recovered *emm* type 1.0 (isolate 101910) is more adapted to initiating an infection  
193 in the joint more quickly.

194

195 **Concentration and activity of secreted SLO has significant impact on virulence *in vivo***

196 To investigate the effect of secreted SLO on virulence *in vivo*, we tested the amount and activity  
197 of SLO released into the challenge inoculum (prior to infection of mice) of *emm* type 1.0



198 (isolate 101910) and *emm* type 32.2 (isolate 112327). At equivalent CFU challenge inoculum  
199 ( $1 \times 10^8$  per 50  $\mu$ l), isolate 112327 had significantly higher SLO concentration ( $p = 0.012$ )  
200 (Figure 5A) and haemolytic activity ( $p = 0.01$ ) (Figure 5A) than isolate 101910. This had a  
201 direct effect on survival *in vivo*, where mice infected with isolate 112327 all died from their  
202 infections, while those infected with isolate 101910 all survived (Figure 5C).

203

204 To further investigate the effect of secreted SLO on infection dose and survival, the  
205 supernatants between isolates 112327 and 101910 were swapped prior to infection of the mice.  
206 Infection doses were prepared in 1 ml of PBS, incubated at room temperature for 30 minutes,  
207 immediately prior to infection bacteria were pelleted by centrifugation and the supernatants of  
208 the two challenge doses were swapped. Mice were infected with either isolate 112327 bacteria  
209 re-suspended in supernatant from isolate 101910 challenge dose or isolate 101910 bacteria re-  
210 suspended in supernatant from isolate 112327 challenge dose. In contrast to original challenge  
211 dose infections, the supernatant swap infected mice exhibited the opposite phenotype, whereby  
212 the normally non-lethal isolate 101910, now killed all mice when infected with supernatant  
213 from isolate 112327, and the normally lethal isolate 112327 isolate became less virulent,  
214 leading to only 50% death as compared to 100% death previously (Figure 5C).

215

216 Moreover, we determined the bacterial load in blood 24 h post-infection. As previously  
217 observed, there were no CFUs of isolate 101910 in blood at 24 h, but a significant 4 Log  
218 increase in CFUs was observed when isolate 101910 was infected with the supernatant swap  
219 dose, clearly suggesting that the high concentration of SLO present in isolate 112327  
220 supernatant was enabling proliferation and retention of isolate 101910 in blood as compared to  
221 its normal condition of being cleared from blood (Figure 5D). In contrast, isolate 112327  
222 challenge dose with isolate 101910 supernatant infected mice had significantly lower CFUs in

223 blood at 24 h in comparison to when infected with its original supernatant ( $p = 0.0079$ ) (Figure  
224 5D) suggesting again, that the concentration and activity of SLO is key to virulence *in vivo*,  
225 both in terms of survival and bacterial load.

226

### 227 **SLO deficiency significantly reduces bacterial load and increases *in vivo* survival**

228 To assess the role of SLO in the virulence of *emm* type 32.2 (isolate 112327) *in vivo* we  
229 generated an isogenic SLO deletion mutant where the SLO gene was deleted and replaced by  
230 a spectinomycin resistance gene through allelic exchange. All mice infected intravenously with  
231 112327  $\Delta$ SLO mutant survived till the end of the experiment (96 h post infection), compared  
232 to mice infected with the wild type isolate whom all succumbed to infection by 24h (Figure  
233 6A). The difference in mouse survival can be explained by the bacterial load in blood, which  
234 was 3.5 log lower in the  $\Delta$ SLO mutant by 24h post infection, than that observed in mice infected  
235 with the wild type isolate ( $p = <0.0001$ ) (Figure 6B). Furthermore, the bacterial burden of the  
236 112327  $\Delta$ SLO mutant decreased over time and by 96 h post infection, bacteria were completely  
237 cleared from the blood (Figure 6B). These results indicate that in the absence of the toxin,  
238 bacteria were less able to establish an infection in the blood or were able to translocate  
239 elsewhere. Indeed, as described before during infection with *emm* type 1.0 (isolate 101910),  
240 mice infected with *emm* type 32.2 (isolate 112327)  $\Delta$ SLO mutant also began to show joint  
241 deformities by 24 h. We detected a high bacterial load in the knee joints, contrary to mice  
242 infected with the wild type isolate in which no bacteria in knee joints or deformities were  
243 observed (Figure 6C). Interestingly, we detected no difference in the bacterial burden in the  
244 joints between 112327  $\Delta$ SLO mutant and *emm* type 1.0 (isolate 101910) (Figure 6C), which  
245 demonstrates that the kinetics of the infection was the same across the two different isolates  
246 and suggests that as well as being a key factor necessary and sufficient to virulence *in vivo*,  
247 SLO is also intriguingly the driving factor in determining the phenotypic outcome of infection.

248 **Liposome treatment reduces bacterial load and increases survival**

249 Our previously published work has explored using cholesterol rich liposomes (cholesterol:  
250 sphingomyelin liposomes; 66 mol/% cholesterol) as a method to sequester cholesterol  
251 dependent cytolytins both *in vitro* and *in vivo*<sup>31,32</sup>. We have shown that administration of  
252 cholesterol rich liposomes within 10 h after initiation of infection stopped the progression of  
253 bacteraemia caused by *S. aureus* and *S. pneumoniae*<sup>31</sup> and that liposomes were also able to  
254 bind strongly to SLO<sup>31,32</sup>. Based on this, we now used specially tailored cholesterol rich  
255 liposomes as targets to sequester secreted SLO *in vivo*.

256

257 Liposomes were successful in sequestering the toxin as the concentration of SLO was  
258 significantly lower in *emm* type 32.2 (isolate 112327) supernatant when incubated with  
259 liposomes as compared to non-liposome control ( $p = 0.003$ ) (Figure 7A). When the bacterial  
260 challenge dose was co-incubated with liposomes prior to infection, all mice infected with  
261 liposome treated isolate 112327, survived a further 24 h as compared to non-liposome treated  
262 control challenge dose (Figure 7B) and this extended survival period correlated with reduced  
263 CFU load in blood (Figure 7C). In addition, the effects of giving liposomes as a treatment to  
264 invasive GAS was also considered. A single injection of the liposomal mixture was  
265 administered at 4 h post infection. All mice that were not liposome treated succumbed to  
266 infection by 24 h, in comparison 60% of mice treated with the liposomal mixture survived an  
267 extra 24 h to 48 h (Figure 7D). In line with the differences in survival time, there was a  
268 considerable reduction of the bacterial load in the blood of mice that had been injected with a  
269 single dose of liposomes at 4 h in comparison to no treatment group (Figure 7E). These results  
270 show that a treatment with liposomes reduces the amount of SLO secreted into the extracellular  
271 environment, leading to a considerable reduction of the bacterial burden in the blood of mice  
272 and to attenuation of invasive GAS infection.

## 273 Discussion

274 In this study, we investigated the role of SLO in determining disease phenotype, and found that  
275 differences in production and activity of SLO was central to *in vivo* pathotype and disease  
276 outcome in GAS infections.

277

278 In summary, we found that SLO production and activity drove two very distinct *in vivo*  
279 pathotypes; *emm* type 32.2 isolates which produced SLO in high levels and with high activity  
280 and *emm* type 1.0 isolates, which were the exact opposite with low levels of SLO production  
281 and of low activity. This correlated directly with their *in vivo* pathotype i.e. high virulence in  
282 bacteraemia models accompanied by short host survival (*emm* type 32.2) and low virulence in  
283 chronic septic arthritis models accompanied by long term host survival (*emm* type 1.0). Indeed,  
284 we found that the levels and activity of SLO at time of initial infection, determined the disease  
285 phenotype, with high levels of SLO driving invasive disease and low levels sustaining chronic  
286 joint infections. When removing SLO from the *in vivo* environment, either by gene deletion or  
287 by significantly reducing SLO (by supernatant swap or liposome sequestration method), we  
288 were able to demonstrate a complete reversal in the *in vivo* pathotypes of these *emm* isolates,  
289 whereby normally bacteraemia causing *emm* type 32.2 isolates could be made to translocate  
290 into joints rather than killing their hosts, and septic arthritis causing *emm* type 1.0 isolates could  
291 be made highly invasive, highlighting the crucial role of SLO in determining disease phenotype  
292 and outcome *in vivo*.

293

294 SLO is a major virulence factor for GAS, expressed by nearly all strains, and with amino acid  
295 sequence homology highly conserved between strains<sup>33</sup>. Multiple roles in pathogenicity *in vivo*  
296 have been attributed to SLO, and recent studies have shown that SLO is important in the  
297 evasion of the host response via a number of mechanisms. Timmer *et al.*, demonstrated that

298 GAS induces rapid macrophage and neutrophil apoptosis due to the effects of SLO<sup>24</sup>, and  
299 further work in the field has demonstrated that SLO rapidly impairs neutrophil oxidative burst  
300 preventing the bactericidal action of neutrophils<sup>34</sup>. The effects of the general presence of  
301 secreted SLO in the blood stream has been less well studied however, although it has been  
302 implicated in driving inflammation, including the well documented evidence on activation of  
303 the NLRP3 inflammasome<sup>35</sup>, hence, it would therefore seem likely that SLO production and  
304 activity is important for GAS in invasive bacteraemia infections yet there has been no studies  
305 to date to show that SLO itself could be driving disease phenotype *in vivo*.

306

307 Although the SLO gene is highly conserved among all *emm* types of GAS, studies have shown  
308 that there are differences in the expression of the SLO gene which regulates the production of  
309 secreted SLO<sup>35</sup>, and that specific invasive variants can be isolated post *in vivo* passage<sup>13</sup>. In  
310 addition to this, it has been shown that *in vivo* conditions can result in differential expression  
311 of certain proteins; a study looking at exotoxins SpeA and SpeB found that *in vivo* host and/or  
312 environmental signals induced SpeA gene expression and suppressed SpeB expression that  
313 could not be induced under *in vitro* conditions<sup>15</sup>.

314

315 This study demonstrates that SLO levels and activity determine invasiveness or chronicity  
316 during infection. The role of SLO was further investigated using supernatant switching, an  
317 SLO-deficient mutant and SLO sequestration by cholesterol rich liposomes. When the  
318 supernatant of isolate 112327 was replaced with isolate 101910 supernatant, the amount of  
319 SLO in the challenge inoculum was significantly reduced and 50% of the mice challenged were  
320 able to clear the infection, a delayed invasive phenotype was observed with mortality at 48 h  
321 instead of 24 h with 112327 and its original supernatant. This demonstrated that without the  
322 initial high SLO concentration in the challenge inoculum there is an attenuation of virulence.

323 The bacteria may secrete SLO during the infection but the initial challenge concentration  
324 remains the key determinant resulting in clearance when concentrations are low and increased  
325 virulence with higher concentrations. Interestingly, when we reversed this experiment and used  
326 the supernatant from the challenge inoculum of high SLO secreting isolate 112327 and co-  
327 infected that with isolate 101910, we saw a complete change in the clinical phenotype, whereby  
328 isolate 101910 was now able to successfully proliferate in the blood resulting in host death.  
329 Taking both of these results together, they indicate that the amount of SLO that is initially  
330 secreted is key to virulence in the early stages of infection, and it is possible for the host to  
331 successfully clear the bacteria when SLO concentrations are low. Our data also shows that the  
332 ability of the mice to survive infection is linked with the ability of the bacteria to proliferate.  
333 Early studies on SLO indicated that it was toxic when injected directly in an animal model<sup>28,36</sup>,  
334 in our study administering the supernatant alone into the mice without any bacteria did not  
335 have a fatal effect. The difference with our study could be due to early studies using  
336 supraphysiological concentrations of purified SLO and/or purified SLO preparations  
337 contaminated with LPS.

338

339 To consider how the complete removal of SLO affects the progression of invasive infection,  
340 an isogenic SLO deletion mutant of isolate 112327 was made. Our results demonstrate that  
341 mice infected with the SLO mutant had a significantly higher rate of survival than mice infected  
342 with its parent wild type bacteria. None of the mice infected with the mutant succumbed to  
343 infection where as 100% of mice infected with the wildtype died at 24 h. The SLO mutant  
344 began to be cleared from the blood as early as 24 h and was completely cleared by 96 h.  
345 Surprisingly, we found that the SLO deficient mutant sequestered in the knee joints causing  
346 septic arthritis as previously seen during infection with the low SLO secreting isolate 101910.  
347 The results clearly show that GAS strains lacking SLO and or low SLO producing GAS strains

348 are severely impaired in their ability to cause bacteraemia and that lack (or reduced levels) of  
349 SLO enables the bacteria to accumulate within host joints.

350

351 There have been a number of previous studies using SLO mutants which have found that  
352 virulence is attenuated, although the relative importance of SLO would appear to be dependent  
353 on disease model used<sup>23,28,29,37</sup>. For example, Limbago *et al.*, used a subcutaneous invasive  
354 skin infection model to study the virulence of SLO-deficient mutants, where they found that  
355 although there were increased survival times of mice infected with SLO deficient strains, the  
356 absence of SLO itself did not limit dissemination from the wound into the vasculature<sup>28</sup>. In  
357 contrast to this, a later study by Sierig *et al.*, found that during a skin infection model initiated  
358 by intraperitoneal infection there were no changes to survival using an SLO deficient mutant  
359<sup>23</sup>. A more recent study looking at the emergence of an invasive *emm* type 89.0 clade, showed  
360 that elevated SLO producers are significantly more virulent than low SLO producers<sup>25</sup>. Based  
361 on our findings here, we speculate that the low production of SLO (or SLO deficiency) prevents  
362 the ability of GAS to cause bacteraemia while enhancing its capability to translocate into the  
363 joints. Low SLO secreting isolate 101910 which effectively colonises the joints, adapts further  
364 to the joint by selecting for low secreting SLO variants. This is a selection pressure applied  
365 from environmental signals in the joint as when the isolate is recovered from the joints and  
366 placed under growth conditions *in vitro* it reverts to producing significantly more SLO (Figure  
367 4C). Moreover, deletion of SLO in isolate 112327 resulted in a complete reversal of *in vivo*  
368 phenotype, whereby these SLO deficient isolates now caused septic arthritis.

369

370 The exact mechanism by how GAS infects the joint is not clear. The general mechanism of  
371 joint colonisation begins with haematogenous entry into the vascularised synovium. Once  
372 bacteria are in the joint space the low fluid shear conditions provide a unique opportunity for

373 bacterial adherence and infection<sup>38</sup>. Different strains of bacteria that commonly infect the joint  
374 including GAS and others such as *S. aureus* have varying degrees of tropism to the joint,  
375 thought to be due to differences in adherence characteristics and toxin production<sup>38</sup>. We have  
376 previously shown that isolate 112327 is an outbreak strain with characteristics that suggest it  
377 is hypervirulent, e.g. it has 19 extra genes, five of which are associated with an increase in  
378 virulence<sup>39</sup>. We have shown in this current study that isolate 112327 is more virulent in an  
379 invasive bacteraemia model and produced significantly more SLO which is likely to be one of  
380 the causes of its increased capacity to cause host death.

381

382 Infection with isolate 112327 results in uncontrolled bacterial proliferation in blood and rapid  
383 progression into sepsis. On the other hand, isolate 101910 which was isolated from a patient  
384 with septic arthritis and produces low concentrations of SLO, can be reduced to even lower  
385 concentrations after further selection from the joint. This implies that decreased production of  
386 SLO is beneficial during infection in the joint. Reduced or no expression of SLO could have a  
387 protective effect for the pathogen, as SLO is immunogenic and avoiding host immune cell  
388 detection could thereby prevent immune activation and clearance, allowing GAS to continue  
389 to colonise the joint<sup>21</sup>.

390

391 The results presented here have important implications for our understanding of GAS  
392 pathogenesis. We conclude that levels and activity of SLO is key to determining whether GAS  
393 infection follows an highly invasive and virulent pattern leading to host death or whether it  
394 follows a chronic pattern of long term joint infection. The fact that these disease phenotypes  
395 are not fixed is highly interesting, as it suggest that GAS is highly sensitive to environmental  
396 signals and can change its phenotype rapidly. Indeed, by artificially effecting SLO levels, we  
397 have shown that one disease phenotype can easily be switched into another. This has significant



398 implications for therapy and vaccines as anti-SLO based treatments may not be the complete  
399 answer to protection against all forms of GAS infection.

400

## 401 **Materials and methods**

### 402 **Epidemiological study design and collection of isolates**

403 As previously published in Cornick *et al.*, between January 2010 to September 2012, the  
404 Respiratory and Vaccine Preventable Bacteria Reference Unit (RVPBRU) in the United  
405 Kingdom confirmed a total of 14 cases of *emm* type 32.2 invasive GAS in the Merseyside area.  
406 Over the same time period, 30 non-*emm* type 32.2 invasive GAS infections were collected  
407 alongside 20 non-invasive pharyngitis GAS isolates supplied by the Royal Liverpool  
408 University Hospitals Trust and Alder Hey Children's Hospital <sup>30</sup>. The Merseyside outbreak  
409 *emm* type 32.2 isolates (n = 14) were selected for this study alongside a selection of non-*emm*  
410 type 32.2 isolates. Invasive (n = 2) and non-invasive (n = 2) of each *emm* type 6.0 and *emm*  
411 type 89.0 isolates were selected and an additional well studied invasive *emm* type 1.0 isolate.  
412 All isolates were stored in Microbank™ beads prior to study.

413

### 414 **Bacterial culture conditions**

415 Isolates were routinely grown on blood agar base (Oxoid) supplemented with 5% fresh horse  
416 blood and incubated overnight at 37°C in a candle jar. Liquid cultures were prepared in Todd  
417 Hewitt broth with 0.5% yeast extract and 0.5% glucose (THYG) and grown overnight at 37°C.  
418 Stocks of GAS in exponential growth phase were prepared by inoculating THYG broth with  
419 overnight cultures (1:40), and incubating at 37°C for 3-4 h. Glycerol was added (20% v/v) and  
420 stocks were stored at -80°C.

421

422

### 423 **Measurement of capsular thickness**

424 Capsule thickness was measured using the FITC-dextran zone of exclusion method, as  
425 previously described, with minor modifications<sup>40</sup>. Exponential phase cultures were centrifuged  
426 at 3000 g for 10 minutes, and the pellet re-suspended in PBS. 10 µl of bacterial suspension was  
427 mixed with 1 µl of 2000 kDa FITC-dextran (Sigma-Aldrich) and pipetted onto a microscope  
428 slide. The Nikon Eclipse 80i fluorescence microscope (100x magnification) was used to view  
429 the slides and photographs were taken using a Hamamatsu C4742-95 camera. ImageJ was used  
430 to determine the zone of exclusion (area in pixels), a value proportional to capsular thickness.

431

### 432 **Complement deposition**

433 The complement deposition assay was based on a previously published method<sup>41</sup>. Briefly,  
434 bacteria was added to BHI broth, incubated at 37°C for 15 minutes, and centrifuged. The  
435 supernatant was removed and the pellet was washed and re-suspended for incubation in PBS  
436 with 20% human serum (pooled from five individuals) and 1% gelatin veronal buffer. After  
437 washing, they were re-suspended in mouse-anti-human-C3 in PBS (Abcam) and incubated at  
438 37°C for 30 minutes. Washing was repeated, and the contents were re-suspended in anti-Mouse  
439 IgG2a-APC in PBS (EBioscience) and incubated at 4°C for 30 minutes in the absence of light.  
440 After washing, the remaining bacteria were re-suspended in PBS and incubated with thiazole  
441 orange (BD Cell Viability kit). Samples were acquired using the Accuri C6 flow cytometer  
442 (BD).

443

### 444 **Opsonophagocytosis killing assay**

445 The ability of isolates to resist killing by macrophages was measured using an adapted protocol  
446 of a previously published opsonophagocytosis killing assay (OPKA)<sup>42</sup>. J774.2 macrophage  
447 cell line was maintained, as per standard protocols<sup>43</sup>. Bacteria ( $1 \times 10^5$  CFU/ml) were opsonised

448 with IVIg (1:4) in HBSS (plus Ca<sup>2+</sup>/Mg<sup>2+</sup>, 5% FBS) for 20 minutes at 37°C with shaking at  
449 180 rpm. Next, 1×10<sup>5</sup> J774.2 cells were incubated with 5×10<sup>2</sup> CFU of opsonised bacteria and  
450 10 µl of baby rabbit serum complement (37°C, 45 minutes, 180 rpm). The CFU count in each  
451 well was then determined. Percentage killing was calculated from CFU remaining compared  
452 to control samples without J774.2 cells.

453

#### 454 ***In vivo* models of invasive GAS infection**

455 Seven-week-old CD1 mice (Charles River) were intravenously injected with PBS containing  
456 either 10<sup>7</sup> or 10<sup>8</sup> CFU of GAS in exponential growth phase. Following infection, mice were  
457 monitored for physical signs of disease using a standard scoring system<sup>44</sup>. CFU counts were  
458 performed on blood collected at time points by tail bleeding. Mice were humanely culled when  
459 they were scored '++lethargic' and blood tissue was collected for CFU enumeration. To make  
460 passaged stocks two CD1 mice were infected IV with 10<sup>7</sup> bacteria. The mice were monitored  
461 to ensure that 24 h following infection they were at least a score of 1 on the arthritic index, a  
462 scoring system, which evaluates the intensity of arthritis, based on macroscopic inspection. The  
463 mice were humanely culled, the knee joints removed and bacteria recovered to make bacterial  
464 stocks. *In vivo* experimental procedures were reviewed by the University of Liverpool Ethical  
465 and Animal Welfare Committee and carried out under the authority of the UK Home Office  
466 Animals Scientific Procedures Act 1986 (UK Home Office Project Licence number  
467 P86DE83DA).

468

#### 469 **Streptolysin ELISA design and method**

470 Prior to analysis samples were thawed at room temperature. Plates (R&D systems) were coated  
471 with 1 µg/well monoclonal SLO antibody (Abcam) in PBS (Peprotech) at 4°C overnight. Plates  
472 were washed at each step with Peprotech washing buffer. After blocking (Peprotech), samples

473 were added to the wells and incubated for 2 h at room temperature. The plate was washed (x5)  
474 and incubated with rabbit IgG polyclonal anti-SLO antibody (Abcam) for 2 h. Anti-rabbit IgG  
475 alkaline phosphatase conjugate secondary antibody (Abcam) was diluted to 1:5000 in blocking  
476 buffer, and after washing, was added and incubated for 30 mins. After washing, alkaline  
477 phosphatase yellow liquid substrate (PNPP) was added and incubated for 30 mins in the dark,  
478 to stop the reaction 1 M Sodium Hydroxide (NaOH) was used. The plate was loaded on to a  
479 Multiskan Spectrum (Thermo) and the absorbance measured at 405nm. All ELISAs were  
480 carried out with control wells which had all reagents added except samples or diluted SLO.  
481 Duplicate samples of each time point was measured on a single plate and repeated  
482 independently. Each plate contained six two-fold dilutions of a known concentration of SLO.  
483 The results were analysed using Sigma Plot and a standard curve developed to generate  
484 concentrations in ng/ml.

485

#### 486 **Haemolytic activity assay**

487 The haemolytic activity of SLO in culture supernatant was measured as previously described,  
488 with minor modifications<sup>45</sup>. Bacteria-free supernatants were incubated at room temperature  
489 for 10 minutes with 20 mmol/l of dithiothreitol (Sigma-Aldrich). Supernatant was aliquoted  
490 into two tubes; 25 µg of water-soluble cholesterol (inhibitor for SLO activity) was added to  
491 one. Both tubes were incubated at 37°C for 30 minutes, followed by the addition of 2% sheep  
492 erythrocytes/PBS suspension to each sample and further incubation at 37°C for 30 minutes.  
493 PBS was added to each tube the samples were centrifuged at 3000 x g for 5 minutes. Each  
494 sample was transferred to a 96-well plate and the OD<sub>541nm</sub> was measured.

495

496

497

#### 498 **Generation of *slo* deletion GAS mutant**

499 An isogenic SLO knockout mutant of strain *emm* type 32.2 isolate 112327 was constructed  
500 through double-crossover allelic replacement of SLO with *aad9* (encoding spectinomycin  
501 resistance). Regions directly upstream and downstream of SLO (~ 1000 bp each) were  
502 amplified by PCR using primers SLO112327-up-F and SLO112327-up-R, SLO112327-down-  
503 F and SLO112327-down-R respectively, which introduced BamHI restriction sites into the  
504 PCR products. These fragments were stitched together in a second round of PCR using primers  
505 SLO112327-up-F and SLO112327-down-R, generating a 2 kb fragment with a central BamHI  
506 site, which was then ligated into pGEM-T vector (Promega), generating pGEM-T- $\Delta$ slo-2kb.  
507 The plasmid was transformed into *E. coli* DH5 $\alpha$  competent cells (ThermoFischer Scientific).  
508 The *aad9* gene was amplified by PCR using primers *aad9*-F and *aad9*-R. The PCR product was  
509 subcloned into pGEM-T- $\Delta$ slo-2kb at the BamHI restriction site, generating pGEM-T-  
510  $\Delta$ slo::*aad9*, which interrupted the *slo* fragment, providing a means of positive selection of  
511 transformants. The generated plasmid was transformed into *emm* type 32.2 isolate 112327 by  
512 electroporation as previously described<sup>46</sup>. Transformants were recovered on THY agar  
513 supplemented with spectinomycin (100  $\mu$ g/mL) at 37°C in a candle jar for up to 72 h. SLO  
514 deletion was identified by PCR and the PCR products were sequenced to confirm authenticity  
515 of the insertion.

516

#### 517 ***In vivo* invasive model- switching supernatant of isolates**

518 Frozen bacterial stocks were thawed at room temperature and 10<sup>7</sup> bacteria were prepared in 1  
519 ml PBS. After 30 mins both strains were centrifuged at 14,000 x g for 2 mins, the supernatant  
520 from *emm* type 32.2 (isolate 112327) was used to re-suspend *emm* type 1.0 (isolate 101910)  
521 bacteria and the supernatant from *emm* type 1.0 (isolate 101910) was used to re-suspend *emm*  
522 type 32.2 (isolate 112327) bacteria. Mice were immediately infected. The supernatants were

523 analysed using the SLO-ELISA to measure the amount SLO present in ng/ml. Mice were  
524 humanely culled when they were scored '++lethargic' and blood tissue was collected for CFU  
525 enumeration.

526

### 527 **Liposomes**

528 Liposomes were generated with cholesterol and sphingomyelin from egg yolk from Sigma and  
529 dissolved in chloroform at 100 and 50mg/ml respectively. Lipids were mixed together  
530 with cholesterol at 66 mol/% proportion and then evaporated with nitrogen gas for 30min. For  
531 Cholesterol: Sphingomyelin (Ch:Sm) large and small liposomes, the hydration was made by  
532 addition of PBS (ThermoFisher scientific) and incubated at 55°C for 30 mins with vortexing.  
533 To obtain small unilamellar particles, the liposome preparation was then subsequently  
534 sonicated for 30min at 4°C. To eliminate carboxyfluorescein, the preparation was diluted in  
535 PBS and applied to a Sephadex G-25 column in PD-10 (GE Healthcare). Particle concentration  
536 and size distribution of the liposomes generated were evaluated using the NanoSight NS300  
537 instrument (Malvern, UK) and using Nanoparticle Tracking Analysis (NTA) software.

538

### 539 **Data analysis**

540 Statistical analysis was carried out using the GraphPad Prism<sup>®</sup> version 5 statistical package  
541 (GraphPad Software, Inc. <http://www.graphpad.com>). The statistical significance according to  
542 the p-values were summarised as follows: \*p-value<0.05, \*\*p-value<0.01, \*\*\*p-value<0.005  
543 and \*\*\*\*p-value<0.001.

544

545

546

547

548 **Author Contributions**

549 NF and AK conceived, designed and supervised the study and contributed equally throughout.

550 JC, MB, MA, SP, MP and GP performed experiments. WAP and GP provided reagents. JC,

551 NF and AK analysed data. JC and AK wrote the paper with input from all authors.

552 **Competing interests**

553 All authors: No potential conflicts of interest.

554

555 **The Paper Explained**

556 The shifting epidemiology of *Streptococcus pyogenes* (GAS) infections globally over the past

557 decade has been punctuated by *emm* type emergence and localised outbreaks of severe invasive

558 disease. Within *emm* types there is diversity of possible clinical outcomes, however, the basis

559 of these varied clinical phenotypes is not well understood. To address this question, we

560 investigated the role of GAS virulence and its host interactions. We discovered that streptolysin

561 (SLO) can control disease outcome towards either acute pro-inflammatory or chronic disease

562 phenotypes. The specific importance of these results are significant as while neutralisation of

563 SLO activity will reduce severe invasive disease, this carries a risk of the promotion of chronic

564 inflammatory conditions such as septic arthritis.

565

566

567

568

569

570

571

572

## 573 **References**

- 574 1 Carapetis, J. R., Steer, A. C., Mulholland, E. K. & Weber, M. The global burden of  
575 group A streptococcal diseases. *The Lancet. Infectious diseases* **5**, 685-694,  
576 doi:10.1016/s1473-3099(05)70267-x (2005).
- 577 2 Stevens, D. L. Invasive group A streptococcus infections. *Clinical infectious diseases :*  
578 *an official publication of the Infectious Diseases Society of America* **14**,  
579 doi:10.1093/clinids/14.1.2 (1992).
- 580 3 Walker, M. J. *et al.* Disease manifestations and pathogenic mechanisms of group a  
581 Streptococcus. *Clinical microbiology reviews* **27**, 264-301, doi:10.1128/cmr.00101-13  
582 (2014).
- 583 4 Cunningham, M. W. Pathogenesis of group A streptococcal infections. *Clinical*  
584 *microbiology reviews* **13**, 470-511 (2000).
- 585 5 Musser, J. M. & Shelburne, S. A., 3rd. A decade of molecular pathogenomic analysis  
586 of group A Streptococcus. *The Journal of clinical investigation* **119**, 2455-2463,  
587 doi:10.1172/jci38095 (2009).
- 588 6 Sriskandan, S. & Altmann, D. M. The immunology of sepsis. *The Journal of Pathology*  
589 **214**, 211-223, doi:10.1002/path.2274 (2008).
- 590 7 Kotb, M. *et al.* An immunogenetic and molecular basis for differences in outcomes of  
591 invasive group A streptococcal infections. *Nature Medicine* **8**, 1398,  
592 doi:10.1038/nm1202-800 [https://www.nature.com/articles/nm800 - supplementary-](https://www.nature.com/articles/nm800 - supplementary-information)  
593 [information](https://www.nature.com/articles/nm800 - supplementary-information) (2002).
- 594 8 Beall, B., Facklam, R. & Thompson, T. Sequencing emm-specific PCR products for  
595 routine and accurate typing of group A streptococci. *Journal of clinical microbiology*  
596 **34**, 953-958 (1996).
- 597 9 Steer, A. C., Lamagni, T., Curtis, N. & Carapetis, J. R. Invasive group a streptococcal  
598 disease: epidemiology, pathogenesis and management. *Drugs* **72**, 1213-1227,  
599 doi:10.2165/11634180-000000000-00000 (2012).



- 600 10 Molinari, G. & Chhatwal, G. S. Invasion and Survival of Streptococcus pyogenes in  
601 Eukaryotic Cells Correlates with the Source of the Clinical Isolates. *The Journal of*  
602 *infectious diseases* **177**, 1600-1607, doi:10.1086/515310 (1998).
- 603 11 Shiseki, M. *et al.* Comparison of pathogenic factors expressed by group A Streptococci  
604 isolated from patients with streptococcal toxic shock syndrome and scarlet fever.  
605 *Microbial pathogenesis* **27**, 243-252, doi:10.1006/mpat.1999.0302 (1999).
- 606 12 Kansal, R. G., McGeer, A., Low, D. E., Norrby-Teglund, A. & Kotb, M. Inverse  
607 Relation between Disease Severity and Expression of the Streptococcal Cysteine  
608 Protease, SpeB, among Clonal MIT1 Isolates Recovered from Invasive Group A  
609 Streptococcal Infection Cases. *Infection and immunity* **68**, 6362-6369,  
610 doi:10.1128/iai.68.11.6362-6369.2000 (2000).
- 611 13 Rezcallah, M. S., Boyle, M. D. P. & Sledjeski, D. D. Mouse skin passage of  
612 Streptococcus pyogenes results in increased streptokinase expression and activity.  
613 *Microbiology* **150**, 365-371, doi:doi:10.1099/mic.0.26826-0 (2004).
- 614 14 Raeder, R., Harokopakis, E., Hollingshead, S. & Boyle, M. D. P. Absence of SpeB  
615 Production in Virulent Large Capsular Forms of Group A Streptococcal Strain 64.  
616 *Infection and immunity* **68**, 744-751, doi:10.1128/iai.68.2.744-751.2000 (2000).
- 617 15 Kazmi, S. U. *et al.* Reciprocal, Temporal Expression of SpeA and SpeB by Invasive  
618 MIT1 Group A Streptococcal Isolates In Vivo. *Infection and immunity* **69**, 4988-4995,  
619 doi:10.1128/iai.69.8.4988-4995.2001 (2001).
- 620 16 Smith, T. C., Sledjeski, D. D. & Boyle, M. D. P. Streptococcus pyogenes Infection in  
621 Mouse Skin Leads to a Time-Dependent Up-Regulation of Protein H Expression.  
622 *Infection and immunity* **71**, 6079-6082, doi:10.1128/iai.71.10.6079-6082.2003 (2003).
- 623 17 Sumbly, P., Whitney, A. R., Graviss, E. A., DeLeo, F. R. & Musser, J. M. Genome-wide  
624 analysis of group a streptococci reveals a mutation that modulates global phenotype  
625 and disease specificity. *PLoS pathogens* **2**, e5, doi:10.1371/journal.ppat.0020005  
626 (2006).

- 627 18 Berry, A. M., Yother, J., Briles, D. E., Hansman, D. & Paton, J. C. Reduced virulence  
628 of a defined pneumolysin-negative mutant of *Streptococcus pneumoniae*. *Infection and*  
629 *immunity* **57**, 2037-2042 (1989).
- 630 19 Dramsi, S. & Cossart, P. Listeriolysin O. *a genuine cytolysin optimized for an*  
631 *intracellular parasite* **156**, 943-946, doi:10.1083/jcb.200202121 (2002).
- 632 20 Alouf, J. E. Cholesterol-binding cytolytic protein toxins. *International Journal of*  
633 *Medical Microbiology* **290**, 351-356, doi:[https://doi.org/10.1016/S1438-](https://doi.org/10.1016/S1438-4221(00)80039-9)  
634 [4221\(00\)80039-9](https://doi.org/10.1016/S1438-4221(00)80039-9) (2000).
- 635 21 Chiarot, E. *et al.* Targeted Amino Acid Substitutions Impair Streptolysin O Toxicity  
636 and Group A *Streptococcus* Virulence. *mBio* **4**, doi:10.1128/mBio.00387-12 (2013).
- 637 22 Bensi, G. *et al.* Multi high-throughput approach for highly selective identification of  
638 vaccine candidates: the Group A *Streptococcus* case. *Molecular & cellular proteomics*  
639 *: MCP* **11**, M111.015693, doi:10.1074/mcp.M111.015693 (2012).
- 640 23 Sierig, G., Cywes, C., Wessels, M. R. & Ashbaugh, C. D. Cytotoxic Effects of  
641 Streptolysin O and Streptolysin S Enhance the Virulence of Poorly Encapsulated Group  
642 A *Streptococci*. *Infection and immunity* **71**, 446-455, doi:10.1128/iai.71.1.446-  
643 455.2003 (2003).
- 644 24 Timmer, A. M. *et al.* Streptolysin O Promotes Group A *Streptococcus* Immune Evasion  
645 by Accelerated Macrophage Apoptosis. *Journal of Biological Chemistry* **284**, 862-871,  
646 doi:10.1074/jbc.M804632200 (2009).
- 647 25 Zhu, L., Olsen, R. J., Nasser, W., de la Riva Morales, I. & Musser, J. M. Trading  
648 Capsule for Increased Cytotoxin Production: Contribution to Virulence of a Newly  
649 Emerged Clade of emm89 *Streptococcus pyogenes*. *mBio* **6**, e01378-01315,  
650 doi:10.1128/mBio.01378-15 (2015).
- 651 26 Howard, J. G. & Wallace, K. R. The comparative resistances of the red cells of various  
652 species to haemolysis by streptolysin O and by saponin. *British journal of experimental*  
653 *pathology* **34**, 181-184 (1953).

- 654 27 Halpern, B. N. & Rahman, S. Studies on the cardiotoxicity of streptolysin O. *British*  
655 *Journal of Pharmacology and Chemotherapy* **32**, 441-452 (1968).
- 656 28 Limbago, B., Penumalli, V., Weinrick, B. & Scott, J. R. Role of Streptolysin O in a  
657 Mouse Model of Invasive Group A Streptococcal Disease. *Infection and immunity* **68**,  
658 6384-6390 (2000).
- 659 29 Zhu, L. *et al.* Contribution of Secreted NADase and Streptolysin O to the Pathogenesis  
660 of Epidemic Serotype M1 Streptococcus pyogenes Infections. *The American journal of*  
661 *pathology* **187**, 605-613, doi:<https://doi.org/10.1016/j.ajpath.2016.11.003> (2017).
- 662 30 Cornick, J. E. *et al.* Epidemiological and Molecular Characterization of an Invasive  
663 Group A Streptococcus emm32.2 Outbreak. *Journal of clinical microbiology* **55**, 1837-  
664 1846, doi:10.1128/jcm.00191-17 (2017).
- 665 31 Henry, B. D. *et al.* Engineered liposomes sequester bacterial exotoxins and protect from  
666 severe invasive infections in mice. *Nature Biotechnology* **33**, 81, doi:10.1038/nbt.3037  
667 [https://www.nature.com/articles/nbt.3037 - supplementary-information](https://www.nature.com/articles/nbt.3037-supplementary-information) (2014).
- 668 32 Alhamdi, Y. *et al.* Circulating Pneumolysin Is a Potent Inducer of Cardiac Injury during  
669 Pneumococcal Infection. *PLoS pathogens* **11**, e1004836,  
670 doi:10.1371/journal.ppat.1004836 (2015).
- 671 33 Barnett, T. C. *et al.* Streptococcal toxins: role in pathogenesis and disease. *Cellular*  
672 *microbiology* **17**, 1721-1741, doi:10.1111/cmi.12531 (2015).
- 673 34 Uchiyama, S. *et al.* Streptolysin O Rapidly Impairs Neutrophil Oxidative Burst and  
674 Antibacterial Responses to Group A Streptococcus. *Frontiers in immunology* **6**, 581,  
675 doi:10.3389/fimmu.2015.00581 (2015).
- 676 35 Zhu, L. *et al.* A molecular trigger for intercontinental epidemics of group A  
677 Streptococcus. *The Journal of clinical investigation* **125**, 3545-3559,  
678 doi:10.1172/jci82478 (2015).
- 679 36 Barnard, W. G. & Todd, E. W. Lesions in the mouse produced by streptolysins O and  
680 S. *The Journal of Pathology and Bacteriology* **51**, 43-47,  
681 doi:doi:10.1002/path.1700510108 (1940).

- 682 37 Bricker, A. L., Carey, V. J. & Wessels, M. R. Role of NADase in virulence in  
683 experimental invasive group A streptococcal infection. *Infection and immunity* **73**,  
684 6562-6566, doi:10.1128/iai.73.10.6562-6566.2005 (2005).
- 685 38 Shirliff, M. E. & Mader, J. T. Acute Septic Arthritis. *Clinical microbiology reviews*  
686 **15**, 527-544, doi:10.1128/CMR.15.4.527-544.2002 (2002).
- 687 39 Cornick, J. E. *et al.* Epidemiological and molecular characterization of an invasive  
688 Group A Streptococcus emm32.2 outbreak. *Journal of clinical microbiology*,  
689 doi:10.1128/jcm.00191-17 (2017).
- 690 40 Hathaway, L. J. *et al.* Capsule Type of Streptococcus pneumoniae Determines Growth  
691 Phenotype. *PLoS pathogens* **8**, e1002574, doi:10.1371/journal.ppat.1002574 (2012).
- 692 41 Hyams, C., Tam, J. C. H., Brown, J. S. & Gordon, S. B. C3b/iC3b Deposition on  
693 Streptococcus pneumoniae Is Not Affected by HIV Infection. *PLOS ONE* **5**, e8902,  
694 doi:10.1371/journal.pone.0008902 (2010).
- 695 42 Romero-Steiner, S. *et al.* Standardization of an opsonophagocytic assay for the  
696 measurement of functional antibody activity against Streptococcus pneumoniae using  
697 differentiated HL-60 cells. *Clinical and diagnostic laboratory immunology* **4**, 415-422  
698 (1997).
- 699 43 Lam, J., Herant, M., Dembo, M. & Heinrich, V. Baseline mechanical characterization  
700 of J774 macrophages. *Biophysical journal* **96**, 248-254,  
701 doi:10.1529/biophysj.108.139154 (2009).
- 702 44 Burkholder, T., Foltz, C., Karlsson, E., Linton, C. G. & Smith, J. M. Health Evaluation  
703 of Experimental Laboratory Mice. *Current protocols in mouse biology* **2**, 145-165,  
704 doi:10.1002/9780470942390.mo110217 (2012).
- 705 45 Sumbly, P. *et al.* Evolutionary origin and emergence of a highly successful clone of  
706 serotype M1 group a Streptococcus involved multiple horizontal gene transfer events.  
707 *The Journal of infectious diseases* **192**, 771-782, doi:10.1086/432514 (2005).

708 46 Franklin, L. *et al.* The AgI/II family adhesin AspA is required for respiratory infection  
709 by *Streptococcus pyogenes*. *PLoS One* **8**, e62433, doi:10.1371/journal.pone.0062433  
710 (2013).

711

712

713

714

715

716

717

718

719

720

721

722

723

724

725

726

727

728

729

730

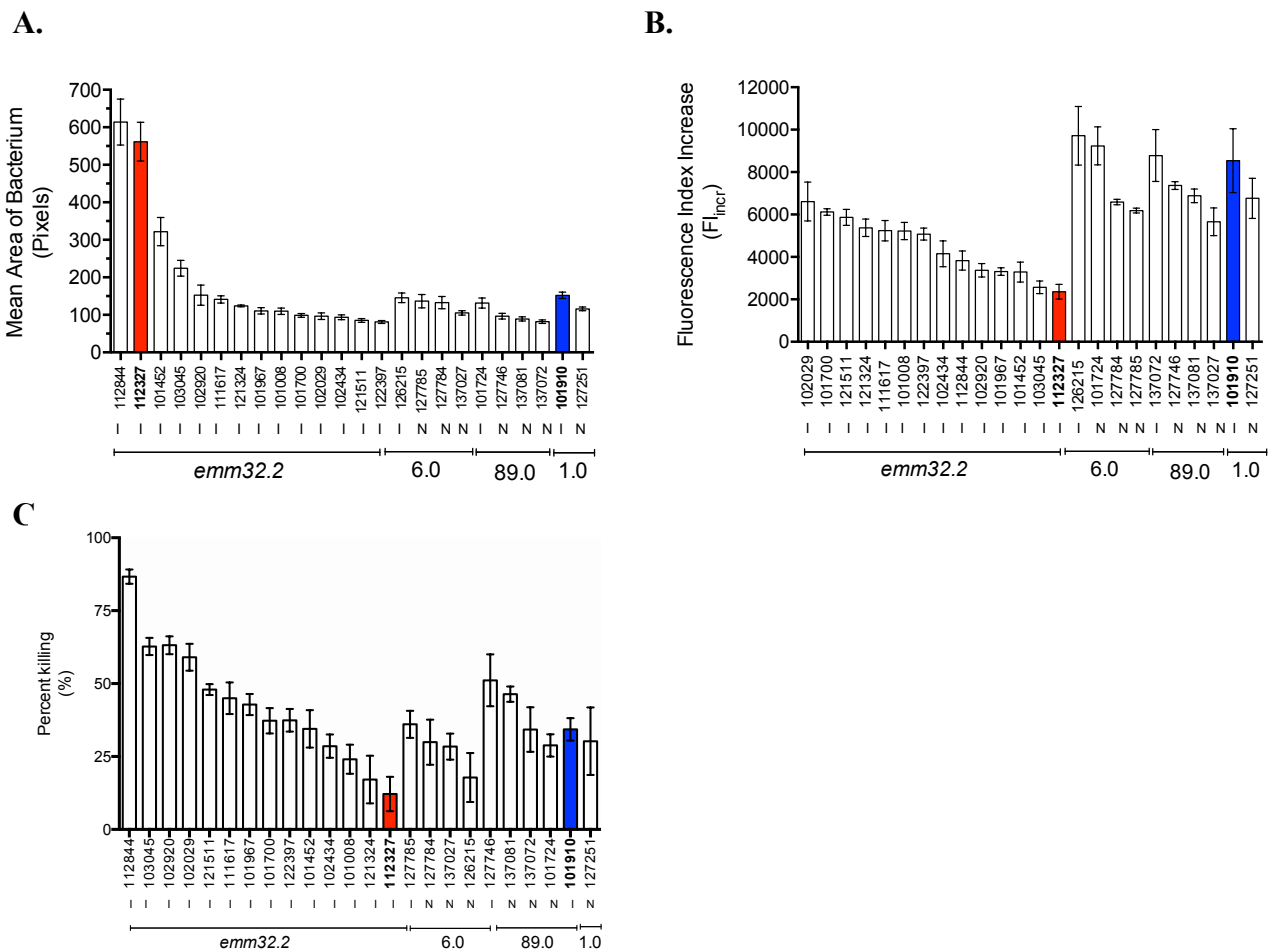
731

732

733

734 **Figures**

735



736

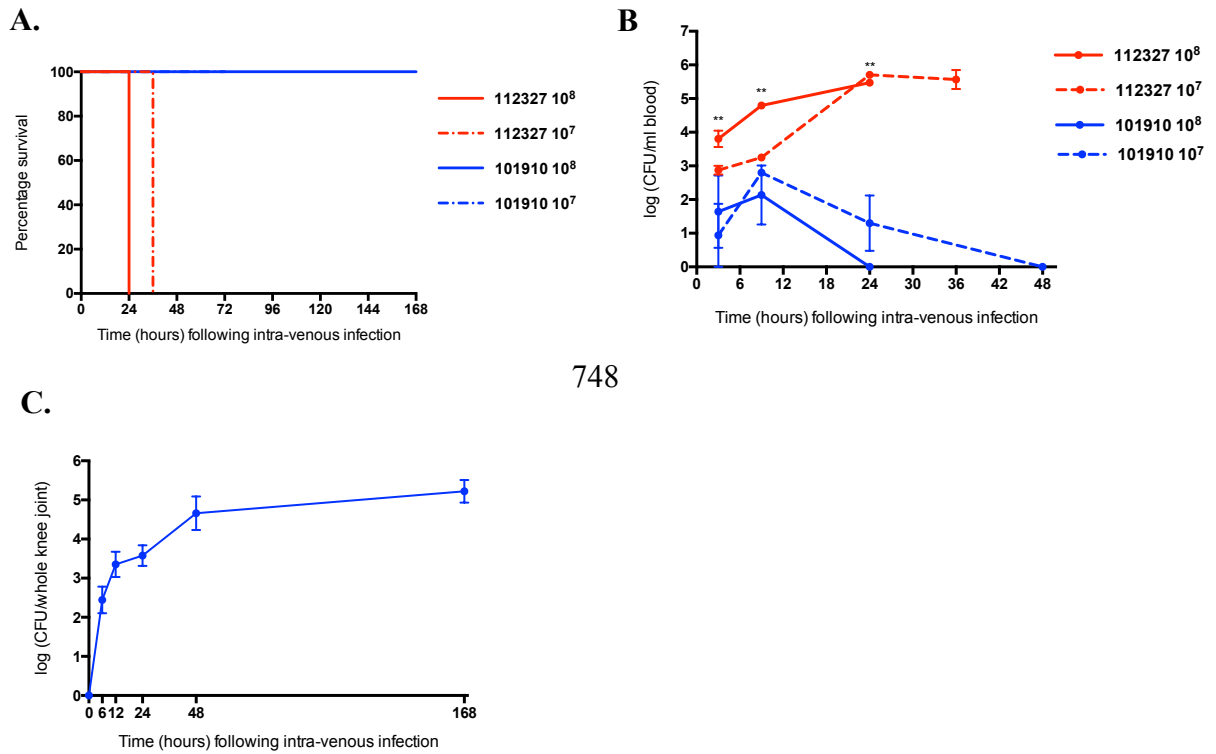
737 **Figure 1 – *In vitro* characterisation of capsule thickness, complement deposition, and**  
 738 **opsonophagocytic killing of invasive and non-invasive *emm* type strains.** A) Capsule  
 739 capsule thickness assay of 24 GAS isolates from 4 different *emm* types. B) Complement deposition  
 740 assay. C) Opsonophagocytic killing assay. Isolates were analysed in triplicate and in three  
 741 independent experiments for each assay, values are presented as mean  $\pm$  S.E.M. I, invasive; N,  
 742 non-invasive. Red and blue columns denote isolates selected for future comparison in mouse  
 743 model experiments.

744

745

746

747



748

753

754 **Figure 2 - *In vivo* characterisation of *emm* type 32.2 (isolate 112327) and *emm* type 1.0**  
755 **(isolate 101910) in a model of invasive GAS infection.** A) Kaplan Meier plots representing  
756 percentage survival of CD1 mice (n = 10 per group) following 10<sup>8</sup> and 10<sup>7</sup> CFU intravenous  
757 infection with *emm* type 1.0 (isolate 101910) and *emm* type 32.2 (isolate 112327). B) The  
758 bacterial CFU in blood for each isolate and infectious dose over time. C) The bacterial CFU in  
759 knee joints of CD1 mice (n = 10, knee joints n = 20) following intravenous infection with 10<sup>7</sup>  
760 CFU (50  $\mu$ l) of *emm* type 1.0 (isolate 101910). \*\*p-value<0.01 when analysed using a one-  
761 way ANOVA followed by a Kruskal- Wallis multiple comparisons test.

762

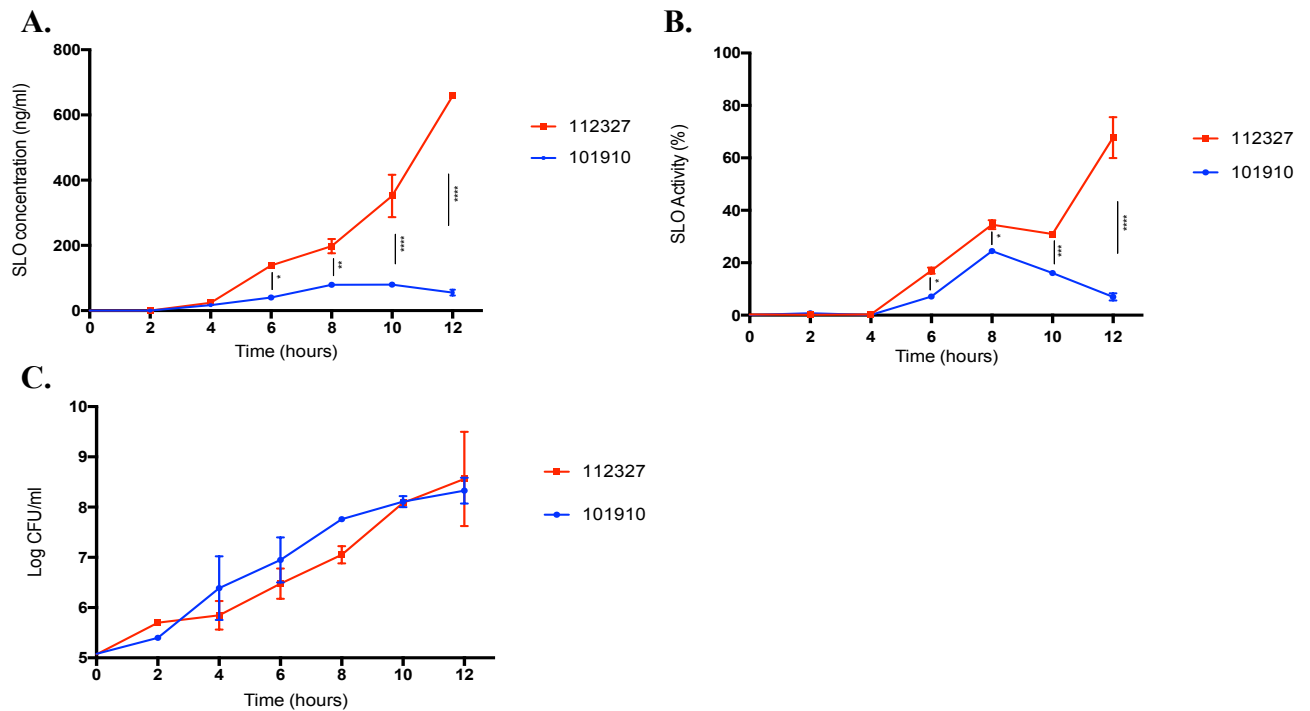
763

764

765

766

767



768

769 **Figure 3 – Comparison of streptolysin production and activity in *emm* type 32.2 (isolate**  
770 **112327) and *emm* type 1.0 (isolate 101910). A) Concentration of streptolysin (ng/ml) secreted**  
771 **into the supernatant by *emm* type 32.2 (isolate 112327) and *emm* type 1.0 (isolate 101910) over**  
772 **time, measured by a custom made SLO-ELISA. B) SLO haemolytic activity C) and growth**  
773 **kinetics of isolates displayed as CFUs. \*p-value<0.05, \*\*p-value<0.01, \*\*\*p-value<0.005, and**  
774 **\*\*\*\*p-value<0.001 when analysed using a two-way ANOVA followed by a Bonferroni’s**  
775 **multiple comparisons correction.**

776

777

778

779

780

781

782

783

784

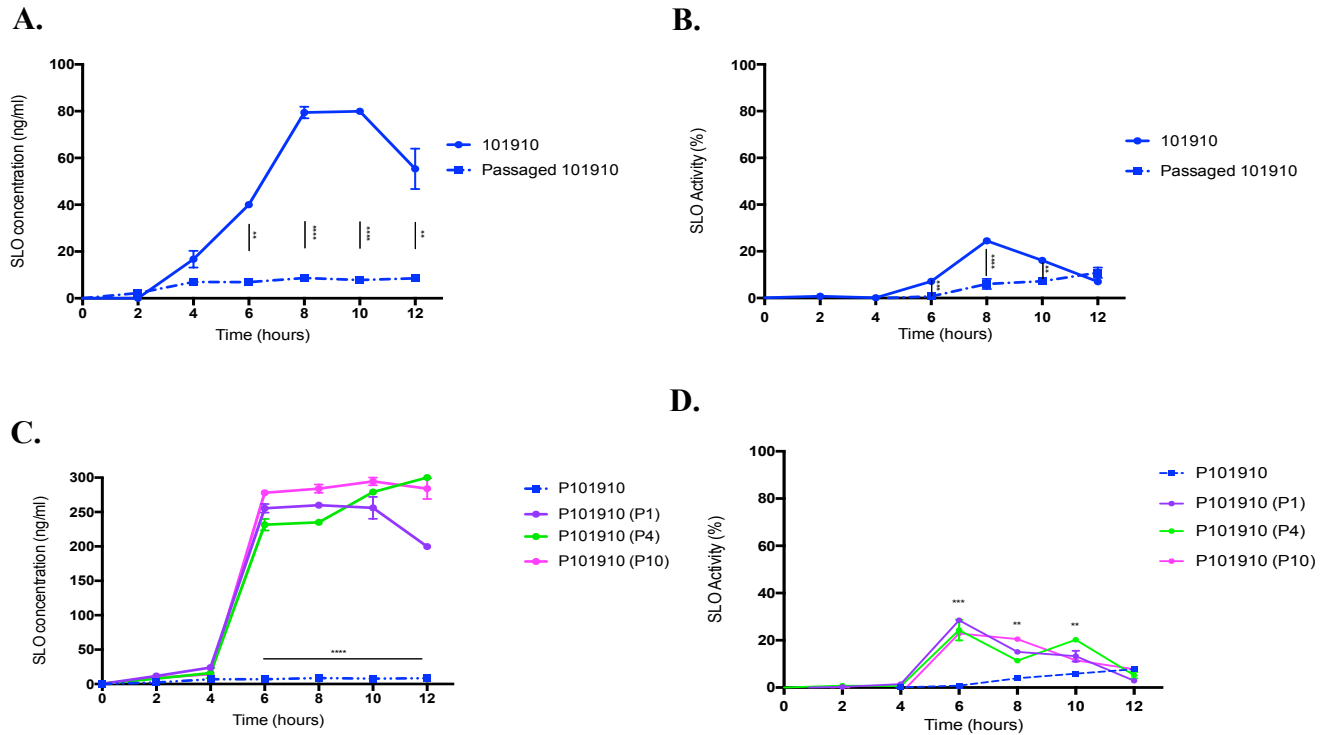
785

786



787

788



789

790 **Figure 4 – Comparison of streptolysin production and activity in *emm* type 1.0 (isolate**  
791 **101910) grown *in vitro* or recovered from *in vivo*.**

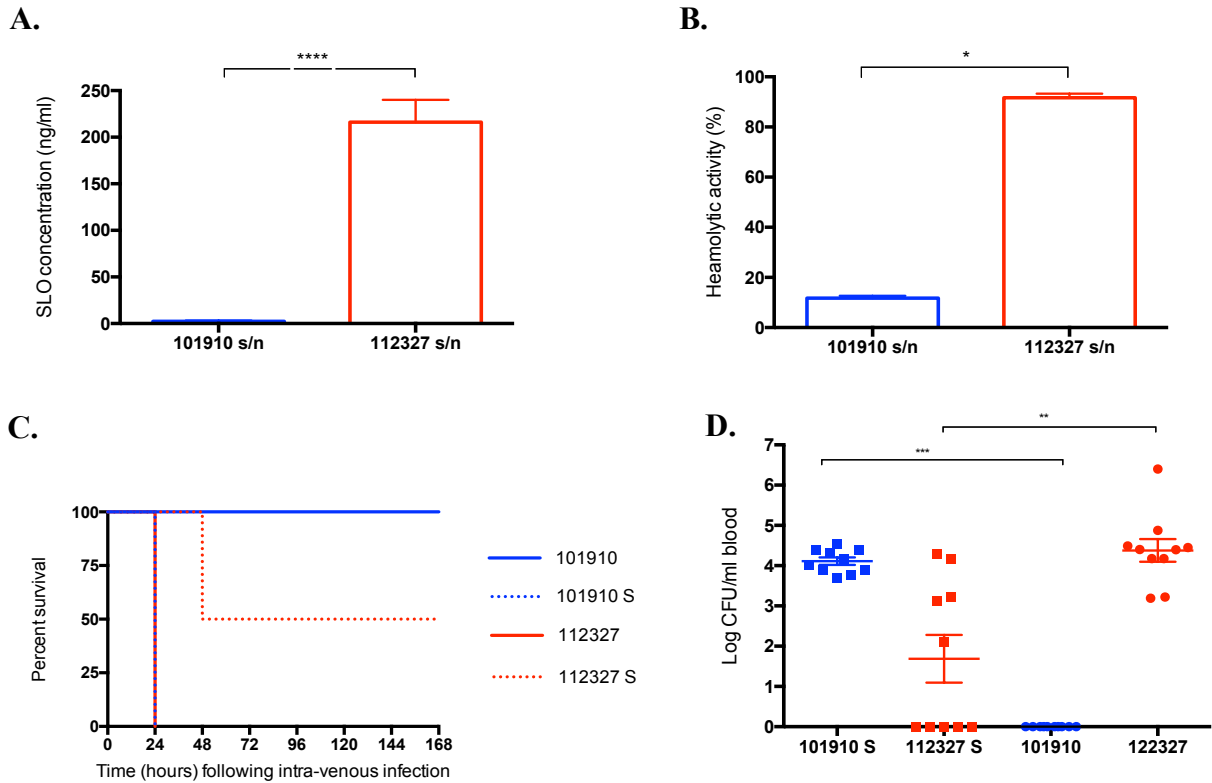
792 A) Concentration of streptolysin (ng/ml) secreted into the supernatant by *emm* type 1.0 (isolate  
793 101910) grown *in vitro* or recovered from knee joints (P101910) and then grown *in vitro*. B)  
794 SLO haemolytic activity. C) After subsequent *in vitro* passaging of *in vivo* recovered P101910  
795 in Todd-Hewitt broth, the concentration of streptolysin (ng/ml) was measured, D) and the SLO  
796 haemolytic activity. \*\*p-value < 0.01, \*\*\*p < 0.005 and \*\*\*\*p-value < 0.001 two-way  
797 ANOVA followed by a Bonferroni's multiple comparisons correction.

798

799

800

801



802

803 **Figure 5 – Effect of concentration and activity of secreted SLO on virulence *in vivo***

804 A) Concentration of streptolysin (ng/ml) and B) haemolytic activity in infection doses of *emm*  
805 type 1.0 (isolate 101910) and *emm* type 32.2 (isolate 112327), when prepared in 1 ml of PBS,  
806 incubated at room temperature for 30 minutes. C) Kaplan Meier survival plots representing  
807 survival of CD1 mice (n = 10 per group) when intravenously infected ( $10^8$  CFU) with isolates  
808 101910 and 112327, and 112327 bacteria re-suspended in supernatant from 101910 challenge  
809 dose (112327 S) or 101910 bacteria re-suspended in supernatant from 112327 challenge dose  
810 (101910 S). D) Bacterial burden in blood 24 hours after infection with isolates 101910 and  
811 112327 and swapped supernatant isolates as above. \*\*p-value < 0.01, \*\*\*p < 0.005 and \*\*\*\*p-  
812 value < 0.001 when analysed using a one-way ANOVA followed by a Kruskal- Wallis  
813 multiple comparisons test.

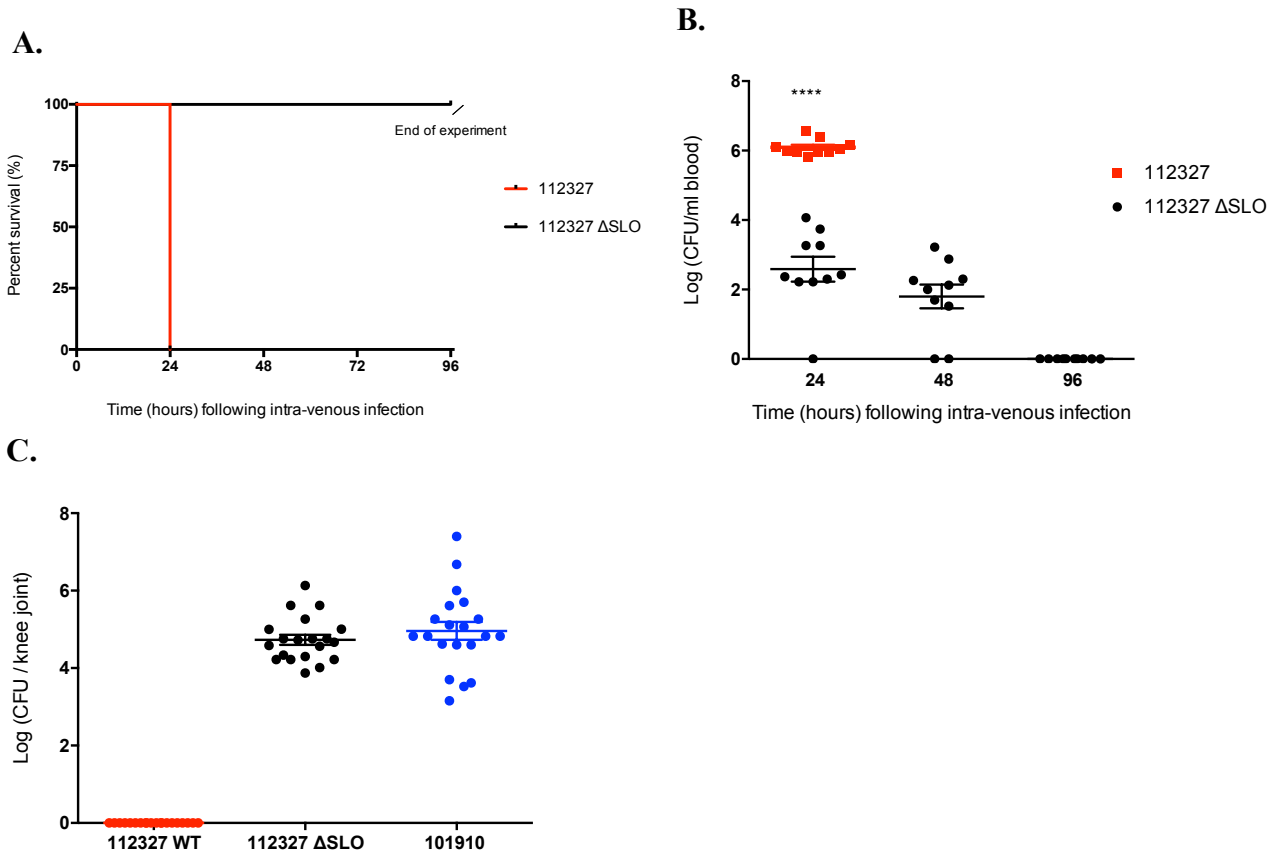
814

815

816

817

818



819

820 **Figure 6 - SLO deficiency increases *in vivo* survival and switches phenotype**

821 A) Kaplan Meier plots representing percentage survival of CD1 mice (n = 10 per group)  
822 following  $10^8$  CFU intravenous infection with isolates *emm* type 32.2 (isolate 112327) and  
823 *emm* type 32.2 (isolate  $\Delta$ SLO 112327). B) The bacterial CFU in blood for each isolate over  
824 time. C) Bacterial load in knee joints (n = 20) at 24 h. \*\*\*\*p-value < 0.0001 when analysed  
825 using a two tailed Mann-Whitney U test.

826

827

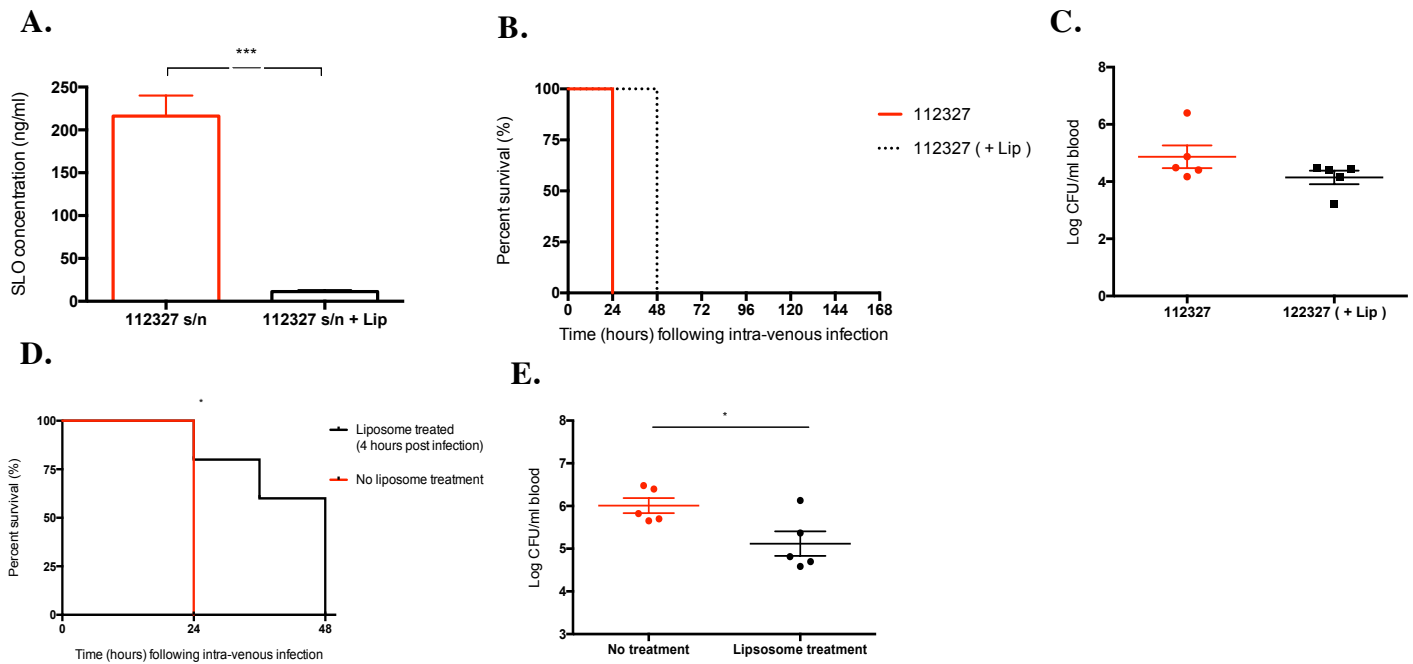
828

829

830

831

832



833

834 **Figure 7 - Liposome SLO treatment reduces bacterial burden and increases survival**

835 A) Concentration of streptolysin (ng/ml) in infection doses of *emm* type 32.2 (isolate 112327)  
836 and *emm* type 32.2 (isolate 112327) after liposome treatment. B) Kaplan Meier survival plots  
837 representing survival of CD1 mice (n = 5) when intravenously infected ( $10^8$  CFU) with *emm*  
838 type 32.2 (isolate 112327) and after treatment of *emm* type 32.2 (isolate 112327) supernatant  
839 with 4  $\mu$ g/ml of liposomes. C) Bacterial burden in blood 24 hours after infection. D) Kaplan  
840 Meier survival plots comparison representing survival of CD1 mice (n = 5 per group) when  
841 intravenously infected ( $10^8$  CFU) *emm* type 32.2 isolate 112327 and after injection of liposomal  
842 mixture 4 h after infection. E) Bacterial burden in blood 24 hours after infection. Survival data  
843 was analysed using the Log-rank (Mantel-Cox) test (\*p < 0.05). Data displayed as mean SEM  
844 and analysed using a two tailed Mann-Whitney U-test (\*p < 0.05, \*\*\*p < 0.005).

845

846